Frontiers in Bioscience Landmark

Front. Biosci. (Landmark Ed) **2026**; 31(7): 52437
https://doi.org/10.31083/FBL52437

Original Research

Nplate (Romiplostim) Restores Blood Counts and Accelerates Wound Healing Following Radiation Combined Injury in Mice

Li Wang[1,2,3,*], Bin Lin[1,2], Min Zhai[1,2], Wanchang Cui[1,4], Lisa Hull[1,2], Alex Zizzo[1], Georgetta Cannon[1], Mang Xiao[1], Juliann G. Kiang[1,4,5,*]

[1]Radiation Combined Injury Program, Armed Forces Radiobiology Research Institute, Uniformed Services University of the Health Sciences, Bethesda, MD 20814, USA
[2]Henry M Jackson Foundation for the Advancement of Military Medicine, Inc., Bethesda, MD 20817, USA
[3]Department of Pathology, Uniformed Services University of the Health Sciences, Bethesda, MD 20814, USA
[4]Department of Pharmacology and Molecular Therapeutics, Uniformed Services University of the Health Sciences, Bethesda, MD 20814, USA
[5]Department of Medicine, Uniformed Services University of the Health Sciences, Bethesda, MD 20814, USA
*Correspondence: li.wang.ctr1@usuhs.edu (Li Wang); juliann.kiang@usuhs.edu (Juliann G. Kiang)
Academic Editor: Graham Pawelec
Submitted: 31 March 2026 Revised: 21 May 2026 Accepted: 17 June 2026 Published: 16 July 2026

Abstract

Background: Exposure to ionizing radiation (IR), particularly when combined with additional trauma such as skin wounding (referred to as radiation combined injury, RCI), results in a synergistic pathology that significantly increases morbidity and mortality compared to isolated radiation injury (RI). While Nplate (romiplostim), a thrombopoietin (TPO) receptor agonist, is a Food and Drug Administration (FDA)-approved medical countermeasure for haematopoietic acute radiation syndrome (H-ARS), its efficacy on RCI is unclear. This study evaluated the mitigative effects of Nplate on 30-day survival, wound healing, and haematopoietic recovery following RCI. **Methods:** Fourteen-week-old female B6D2F1/J mice were exposed to ^{60}Co γ-radiation (9.0 or 9.5 Gy at 0.4 Gy/min) followed by a full-thickness skin wound within one to two h. A single dose of Nplate (30 µg/kg) or vehicle was administered subcutaneously 24 h post-IR. Survival, body weight, and wound closure were monitored for 30 days. On day 30, survivors were euthanized for blood and tissue analysis, including bone marrow histology, colony-forming unit (CFU) assays, complete blood count (CBC), and splenic assessment. **Results:** Nplate significantly improved 30-day survival following 9.5 Gy RI, increasing survival from 30% to 75% ($p = 0.0071$). In contrast, Nplate provided no significant survival improvement in the RCI groups, with 30-day survival rates of 65% at 9.0 Gy ($p = 0.5485$) and 15% at 9.5 Gy ($p = 0.6044$) compared to 75% and 20% in their respective vehicle controls. Despite the lack of survival improvement after RCI, Nplate significantly accelerated wound closure on day 14 after RCI at 9.5 Gy. During the acute phase (Days 1–14), Nplate treatment significantly accelerated healing kinetics, increasing the linear wound healing rate by 54% from 0.124 mm/day to 0.192 mm/day ($p = 0.0205$). Histological analysis revealed that Nplate enhanced bone marrow cellularity, increased megakaryocyte counts, and suppressed IR-induced adipocyte formation. Furthermore, Nplate treatment significantly strengthened functional haematopoiesis, particularly after 9.0 Gy RCI, and stimulated recovery of the splenic lymphoid compartment after both RI and RCI at 9.5 Gy. **Conclusions:** Nplate is a potent mitigator of H-ARS and a stimulator of multi-lineage haematopoietic and tissue regeneration. However, its efficacy in improving survival is limited in RCI, potentially due to exacerbated systemic physiological stress. These results suggest that while Nplate promotes haematopoietic recovery, managing RCI may require a multi-modal approach to address the unique complexities of combined injury, including gastrointestinal (GI)-ARS, systemic inflammation and endothelial dysfunction.

Keywords: haematopoiesis; radiation combined injury; radiation injuries; radiation-mitigated agents; romiplostim; spleen; survival analysis; wound healing

1. Introduction

Exposure to isolated radiation injury (RI) primarily induces dose-dependent damage to the haematopoietic (H) and gastrointestinal (GI) systems [1,2], but when combined with a physical insult like skin wounding, it results in a synergistic pathology that significantly increases morbidity and mortality compared to either injury alone [3,4,5,6,7]. In mouse models, radiation combined injury (RCI) is characterized by a significant decrease in the lethal dose of radiation expected to cause death in 50% of an exposed population within 30 days ($LD_{50/30}$). For example, the $LD_{50/30}$ has been observed to drop from approximately 9.47 Gy (9.31–9.70 Gy) in isolated RI to 9.28 Gy (9.13–9.46 Gy) in RCI groups [8]. RCI typically manifests as a lower survival threshold, an earlier mortality onset, and a significantly delayed wound healing [4,5,8]. This exacerbated lethality is driven by a complex interplay of severe systemic endothelial dysfunction, prolonged systemic inflammation, and impaired granulation tissue formation during the skin wound healing process [8] as well as excessive GI damage caused by RCI [9]. Collectively, these factors hinder the body's ability to combat opportunistic infections from the skin and gut, often leading to sepsis due to the compromised barri-

ers and the suppressed immune response [10,11,12]. The clinical relevance of these findings is underscored by human data from historical events and accidental exposures, which suggest that RCI could account for up to 40–65% of all injuries in mass-casualty nuclear detonation [3,7,13]. Affected victims typically experience shortened latent periods and prolonged, complicated recovery times compared to those presenting with isolated RI [7,14,15].

Nplate, a thrombopoietin (TPO) receptor agonist, has been extensively evaluated across multiple species as a potent medical countermeasure (MCM) for haematopoietic acute radiation syndrome (H-ARS) due to its ability to stimulate the proliferation and differentiation of megakaryocytes and haematopoietic progenitor cells [16]. In mouse models, Nplate administration (typically 30 µg/kg) significantly enhanced survival, restored bone marrow cellularity, and accelerated the recovery of functional haematopoietic lineages, including megakaryocytes and myeloid progenitors [17,18]. Non-human primate (NHP) studies further validated its efficacy, demonstrating that Nplate treatment significantly reduced the duration and severity of radiation-induced thrombocytopenia and neutropenia, thereby improving overall survival when administered within 24 h post-exposure [19]. In humans, while Nplate is Food and Drug Administration (FDA)-approved for immune thrombocytopenia, its clinical application for RI is supported by its ability to bypass the inhibitory effects of the RI-induced myelosuppression, and it is currently stockpiled as a vital therapeutic for mass-casualty under nuclear incidents [19,20].

General clinical observations of TPO agonists suggest they provide a supportive systemic environment for tissue repair, primarily by restoring platelet levels while also exerting broader regenerative and immunomodulatory effects [21,22,23]. Specifically, the kinetics of skin-wound healing might be influenced by TPO agonists through the modulation of local inflammatory responses, angiogenesis, and the release of platelet-derived growth factor (PDGF) [24,25]. These factors were critical for promoting myofibroblast differentiation and collagen deposition, which were essential components of the proliferative phase of healing [25]. While Nplate has been extensively studied in mouse models for accelerating platelet recovery, particularly following radiation or chemotherapy, there is no widely published study explicitly demonstrating that Nplate administration significantly accelerates the skin-wound closure compared to controls in mice.

While Nplate demonstrates a regenerative capacity at the tissue and cellular levels following isolated RI or skin wounding alone, its efficacy in improving overall survival rates in a lethal-dose RCI remains limited. The objective of this study was to evaluate the mitigative effects of Nplate on H-ARS and 30-day mortality following both RI and RCI, as well as the delayed wound healing after RCI. We hypothesized that Nplate would mitigate H-ARS and enhanced 30-day survival after RI and RCI, while also accelerating the skin wound healing process in RCI mice.

2. Materials and Methods

2.1 Animals

Ten-week-old female B6D2F1/J mice were obtained from The Jackson Laboratory (Bar Harbor, ME, USA and Sacramento, CA, USA). The animals were housed in an immunocompromised animal suite within an Association for Assessment and Accreditation of Laboratory Animal Care (AAALAC)-accredited facility overseen by the Department of Laboratory Animal Resources (DLAR) at uniformed services university of the health sciences (USUHS). Following arrival, mice were provided with a three-day acclimation period before the beginning of experimental procedures. At fourteen-week-old, animals were randomly assigned to experimental groups using a weight-stratified randomisation. This process ensured that the average body weight per group was not significantly different prior to the initiation of ionizing radiation or wounding (n = 10 for sham and wound controls; n = 20 for RI and RCI groups). Due to the distinct physical nature of the injuries (e.g., the presence of a visible skin wound in RCI groups compared to RI groups) and the specific drug administration, investigators were not blinded during the outcome assessments. All procedures were conducted in accordance with the Animal Research: Reporting of *In Vivo* Experiments (ARRIVE) guidelines (e.g. animal ethics, sample sizes, housing conditions, humane endpoints). The study protocol was approved by the Institutional Animal Care and Use Committee (IACUC) [5,8,26,27].

2.2 Nplate Administration

Nplate (125 µg/0.25 mL single-dose vial, NDC 55513-223-01, Amgen, Thousand Oaks, CA, USA) was procured through a non-clinical evaluation agreement (NCEA) via the USUHS Pharmacy. The reagent was stored at 4 °C and shielded from light until the time of use. Immediately prior to administration, Nplate was diluted to the target concentration using sterile 0.9% Sodium Chloride (NDC 0990-7953-09, ICU Medical, Inc., Lake Forest, IL, USA). A single dose of 30 µg/kg (0.1 mL per mouse) was administered via subcutaneous (SC) injection 24 h post-total body irradiation (TBI). Control groups received an equivalent volume of sterile saline (Vehicle) following the same route and schedule. The 30 µg/kg dosage was selected based on established efficacy in prior preclinical models of RI [17]. In addition, the 30 µg/kg mouse dose is approximately equivalent to a human dose of 2.44 µg/kg. The clinically approved human dosing range is 1–10 µg/kg. This confirmed that our experimental dose fell well within the clinically relevant range utilized for treating human patients with thrombocytopenia.

2.3 TBI Procedure

TBI was conducted at the Armed Forces Radiobiology Research Institute (AFRRI) ^{60}Co γ-irradiation facility in accordance with previously established protocols. Mice received a bilateral midline tissue dose of either 9.0 Gy or 9.5 Gy, delivered at a dose rate of approximately 0.4 Gy/min [5,8,9,26,27].

2.4 Skin Wounding Procedure

Within 1–2 h following TBI, mice were subjected to a skin wounding procedure performed in accordance with a previously established protocol [5,8,9,27]. Briefly, the wounding procedure consisted of two stages: depilation and skin wounding. Both were under isoflurane (NDC 10019-360-60, Baxter, Deerfield, IL, USA) anesthesia with 3–5% mixed with 100% oxygen at 500–1000 cc/min in the isoflurane chamber. In preparation for wounding, the dorsal fur was shaved using an electric hair clipper two to three days prior to TBI. Within 1–2 h following sham irradiation or TBI, a standardised circular wound (approximately 150–200 mm^2) was created in the anterior-dorsal skin fold of mice in the wound and RCI groups, respectively. The wound was induced using a 70% ethanol (CAS# 64-17-5, Decon Laboratories Inc, King of Prussia, PA, USA)-sterilised stainless steel Arch Punch (9/16-inch/14.3 mm diameter; C.S. Osborne, Harrison, NJ, USA). This approach was employed to ensure consistent injury geometry across all experimental groups. The average initial wound area across all wounded and RCI groups was 187.65 ± 3.49 mm^2 (Mean ± standard error of the mean (SEM), n = 100 mice), as measured on Day 1 post-RCI.

2.5 Experimental Design

The experimental design for the 30-day survival study is summarized in Table 1. A total of 160 mice were utilized, with a sample size of n = 10–20 per group determined by power analysis to ensure statistical significance. Animals were allocated to experimental groups using randomisation via body weight balancing to ensure baseline uniformity. To minimize environmental bias, the spatial arrangement of cages was maintained identically across all IR groups. Throughout the study, including group allocation, experimental procedures, outcome assessment, and data analysis, investigators remained aware of group assignments.

Table 1. Experimental design for a 30-day survival study.

Groups	0.9% Sodium Chloride	Nplate (30 μg/kg)
Sham	n = 10	n = 10
Wound	n = 10	n = 10
9.5 Gy RI	n = 20	n = 20
9.0 Gy RCI	n = 20	n = 20
9.5 Gy RCI	n = 20	n = 20
Total		n = 160

RI, radiation injury; RCI, radiation combined injury.

2.6 Thirty-Day Survival

Animal survival was monitored daily for 30 days after TBI. Health assessments and intervention decisions were guided by the IACUC rodent intervention scoresheet to ensure ethical standards and humane endpoints, as previously described [5,8,9,26,27]. Euthanasia was achieved through CO_2 asphyxiation. The CO_2 flow rate for euthanasia systems is to displace 30–70% of the cage volume/minute. Death occurred within 1–2 min. Once there had been no breath for one min, the animals were then immediately removed from the cage and death was confirmed by cervical dislocation.

2.7 Measurement of Body Weight and Wound Area

Body weight was recorded throughout the study period in accordance with previously established protocols [5,8,27]. To assess wound healing, the wound site was imaged on days 1, 3, 7, 10, 14, 17, 21, 24, and 28 post-TBI using a digital camera (Canon PowerShot G9 X Mark II, Tokyo, Japan). Wound areas were subsequently quantified using Adobe Photoshop (version 27.4.0, San Jose, CA, USA). The percentage of wound closure was calculated using the following formula:

$$\%\text{Wound Closure} = 100\% \times \left[1 - \left(\frac{\text{Wound Area on DayX}}{\text{Wound Area on Day1}}\right)\right]$$

In this equation, "Wound Area on DayX" represents measurements taken at specified time points post-TBI. The wound area on Day 1 was used as the baseline, because these measurements were recorded just before Nplate treatment to fully evaluate its impact on wound healing. The average initial wound area on Day 1 was 187.65 ± 3.49 mm^2 (Mean ± SEM, n = 100 mice). A value of 100% indicates complete wound closure.

In addition, to control potential variations in the baseline size and geometry of the initial injuries, the linear shrinkage of wound margins toward the center was quantified. The linear wound healing rate (WHR) was determined using Gilman's equation [28,29]:

$$\text{Linear wound healing rate (mm/day)} = \frac{\Delta A}{\text{Average perimeter} * \Delta t}$$

ΔA: Change in the wound area between specified time points (mm^2);

Average perimeter: Mean perimeter calculated from the initial and final wound measurements (mm);

Δt: Change in time (day).

This approach provides a normalized assessment of healing kinetics regardless of differences in initial wound shapes.

2.8 Blood and Tissue Collection

On day 30 post-TBI, peripheral blood and multiple tissues, including the sternum, femur, and spleen, were har-

vested from surviving mice in accordance with previously established protocols [5,8,26,27]. Peripheral blood was collected for complete blood count (CBC) analysis, while the sternum and femur were preserved for histological evaluation of bone marrow cellularity and functional progenitor assays, respectively. The spleen was extracted to determine its weight, splenocyte counts, and assess the recovery of the splenic lymphoid compartment.

2.9 Histological Examination of the Sternum

Histological evaluation of the sternum was conducted following previously established protocols [5,26,27]. Megakaryocytes were quantified by counting cells across three distinct fields of view (approximately 130,000 μm^2 each) per animal at 400× magnification. These data are expressed as the mean number of megakaryocytes per defined area. Adipocyte formation was assessed by measuring the total adipocyte area within the same three fields (approximately 130,000 μm^2 each) at 400× magnification. These results are presented as the mean percentage of adipocyte area relative to the total marrow area.

2.10 Clonogenicity Assay

The clonogenic potential of mouse haematopoietic stem and progenitor cells was evaluated using a colony-forming unit (CFU) assay in accordance with previously established protocols [27,30]. Briefly, on day 30 post-irradiation, we isolated bone marrow (BM) cells from the pooled femurs of surviving mice. Total BM cell viability was determined via trypan blue staining. For the clonogenicity assay, we plated BM cells in triplicate (1×10^4 cells/dish) in 35-mm culture dishes (BD Biosciences, San Jose, CA, USA) using 1 mL of MethoCult™ GF+ medium (Catalog #03444, Stemcell Technologies, Cambridge, MA, USA) containing stem cell factor (SCF), interleukin (IL)-3, IL-6, and erythropoietin. Plates were scored for colonies with one colony consisting of fifty or more cells after 8–10 days of incubation (37 °C, 5% CO_2). We scored the CFUs for erythroid (CFU-E), granulocyte-monocyte (CFU-GM), and colony-forming unit—granulocyte, erythroid, macrophage, megakaryocyte (CFU-GEMM) lineages following the manufacturer's instruction. CFU-Total was calculated as the sum of all three lineages.

2.11 CBC

To quantify peripheral blood cell populations, whole blood samples (minimum volume of 15 µL) were collected into ethylenediaminetetraacetic acid (EDTA)-coated microtubes (Cat# 365974, Becton, Dickinson and Company, Franklin Lakes, NJ, USA) to prevent coagulation. Samples were analyzed using an automated clinical hematoanalyzer (Element HT5; Heska, Loveland, CO, USA) in accordance with the manufacturer's instructions and previously established protocols [5,8,26,27].

2.12 Spleen Weight and Splenocyte Quantification

Excised spleens were weighed and splenocytes were quantified in accordance with previously established protocols [26,27]. Splenocyte density, representing the cellular concentration within the splenic tissue, was calculated using the following formula:

$$\text{Splenocyte Density} = \frac{\text{Total Splenocyte Count per Spleen}}{\text{Spleen Weight (mg)}}$$

Splenocyte density was utilized to evaluate the recovery of the splenic lymphoid compartment and to normalize cell counts across varying organ masses following TBI and Nplate treatment.

2.13 Statistical Analysis

Statistical analyses were performed using GraphPad Prism (version 10.6.1; GraphPad Software, La Jolla, CA, USA). Quantitative data are expressed as the mean ± SEM. We used the Shapiro-Wilk test to assess normality and the Brown-Forsythe test to assess homogeneity of variance. Survival distribution was estimated using Kaplan–Meier curves, with statistical differences between treatment cohorts evaluated via the log-rank (Mantel–Cox) test. For comparisons involving multiple experimental groups at a single time point (Day 30), a one-way analysis of variance (ANOVA) followed by Tukey's post hoc test was utilized to identify specific group differences. For data involving multiple time points, a two-way ANOVA followed by Šídák's multiple comparisons test or Fisher's least significant difference (LSD) was employed. For all analyses, statistical significance was predefined as $p < 0.05$ [5,8,26,27].

3. Results

3.1 Nplate Mitigates Lethality Following RI but not RCI

We evaluated the therapeutic efficacy of Nplate on 30-day survival improvement following either RI or RCI. The Log-rank analysis demonstrated a marked difference in Nplate efficacy between the two injuries. In the RI group at 9.5 Gy, administration of Nplate (30 µg/kg) provided a significant survival improvement, increasing the 30-day survival rate from 30% in the vehicle control group to 75% in the Nplate-treated group ($p = 0.0071$; Fig. 1A). In contrast, this therapeutic effect did not extend to the RCI. Following RCI at 9.0 Gy, survival was 75% in the vehicle group compared to 65% in the Nplate group ($p = 0.5485$; Fig. 1B). Similarly, after RCI at 9.5 Gy, the vehicle group reached 20% survival on day 30, while the Nplate-treated group leveled off at 15% ($p = 0.6044$; Fig. 1B). These findings demonstrate that Nplate treatment resulted in no significant difference in 30-day survival compared to vehicle controls at either radiation dose when combined with skin wounding.

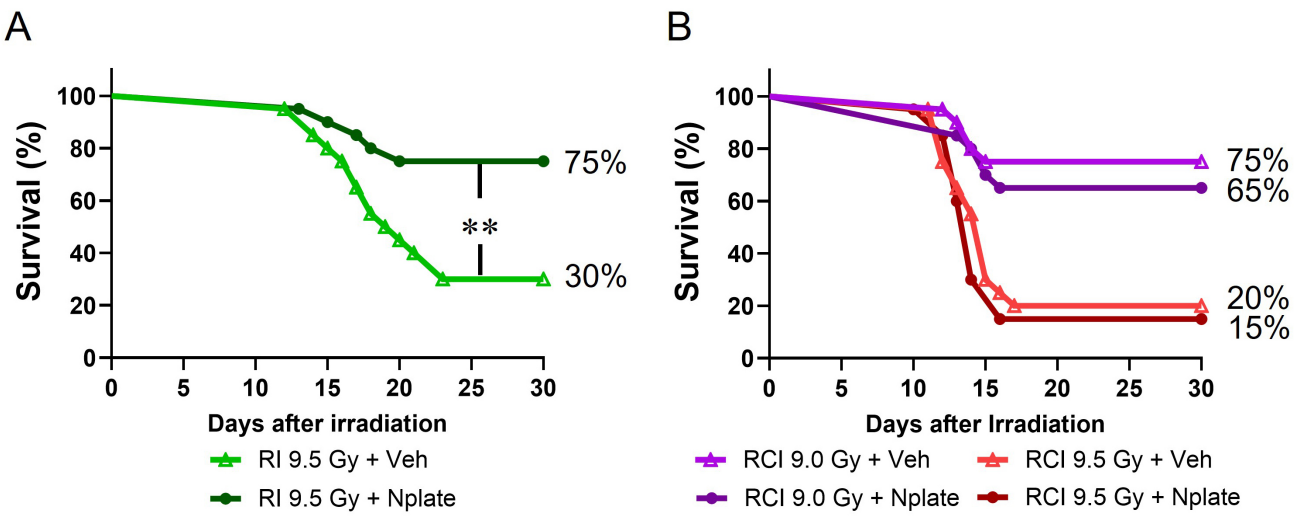

Fig. 1. Nplate improves 30-day survival after RI but fails to provide a therapeutic efficacy after RCI. Kaplan-Meier survival curves of mice (N = 20 per group) following exposure to 9.5 Gy RI or 9.0 Gy/9.5 Gy RCI. (A) RI groups: Mice were exposed to 9.5 Gy RI. Administration of Nplate (30 µg/kg) at 24 h post-RI provided a significant survival improvement, increasing 30-day survival from 30% in the vehicle group (light green) to 75% in the Nplate-treated group (dark green). Statistical significance was determined by Log-rank test (**$p = 0.0071$). (B) RCI groups: Mice were exposed to RCI at either 9.0 Gy or 9.5 Gy. At 9.0 Gy, survival was 75% for the vehicle group (light purple) and 65% for the Nplate group (dark purple). At 9.5 Gy, survival was 20% for the vehicle group (light red) and 15% for the Nplate group (dark red). Nplate failed to provide any survival increase compared to vehicle controls. Veh, Vehicle, sterile saline.

3.2 Nplate Treatment Potentiates Weight Loss Specifically After RCI

To evaluate the physiological impact of treatment, body weight changes were monitored across all experimental groups over a 28-day period. The results indicate that Nplate treatment significantly potentiated body weight loss specifically in RCI groups. In the absence of TBI, Nplate had no adverse effects on body weight. Both the Sham (Fig. 2A) and Wound-only (Fig. 2C) groups treated with Nplate followed growth trajectories nearly identical to their respective vehicle controls. In the RI group at 9.5 Gy (Fig. 2B), Nplate-treated mice showed a similar, if not slightly improved, recovery pattern compared to the vehicle group. However, in the 9.0 Gy RCI group (Fig. 2D), Nplate-treated mice experienced significantly greater weight loss on Day 14 post-TBI compared to vehicle controls ($p = 0.0211$). This effect was even more pronounced in the RCI group at 9.5 Gy (Fig. 2E), where Nplate treatment led to a significantly deeper and more prolonged weight nadir on Day 17 ($p = 0.0036$). While vehicle-treated RCI mice began recovering their body weight after Day 14, the Nplate group remained significantly suppressed till Day 17.

3.3 Nplate Treatment Accelerates Wound Closure After RCI at 9.5 Gy

We monitored the rate of wound closure over a 28-day period after RCI (Fig. 3). The representative wound images are shown in Fig. 3A. In mice subjected to wound alone or RCI at 9.0 Gy, Nplate treatment did not significantly alter the rate of closure compared to vehicle control (Fig. 3B,C). However, following exposure to RCI at 9.5 Gy, Nplate-treated mice exhibited a significantly faster rate of closure on day 14 post-TBI ($p = 0.0097$), compared to vehicle-treated controls (Fig. 3D). Furthermore, as illustrated in Fig. 3E, Nplate administration significantly enhanced wound repair kinetics in the RCI group at 9.5 Gy. Specifically, during the acute healing phase between Day 1 and Day 14, Nplate-treated RCI mice at 9.5 Gy exhibited a 54% increase from 0.124 mm/day to 0.192 mm/day in the linear wound healing rate compared to vehicle-treated controls ($p = 0.0205$). In contrast, during the late remodeling phase between Day 14 and Day 28, the linear wound healing rate showed no significant differences between Nplate and vehicle treatments across the wound-only, 9.0 Gy RCI, or 9.5 Gy RCI groups (Fig. 3F).

3.4 Nplate Treatment Enhances Bone Marrow Cellularity on Day 30 After RI and RCI

Histological and quantitative analysis of sternum bone marrow on Day 30 post-TBI revealed that while radiation (9.5 Gy RI and 9.0/9.5 Gy RCI) significantly decreased megakaryocyte counts and increased adipocyte formation compared to Sham and/or Wound-only controls, Nplate treatment (30 µg/kg) effectively promoted haematopoietic regeneration after RI and RCI (Fig. 4). Representative Hematoxylin and Eosin (H&E) staining demonstrated that Nplate-treated mice in both 9.5 Gy RI and 9.0 Gy RCI groups possessed significantly dense haematopoietic clusters and reduced fatty cells compared to their respective vehicle controls (Fig. 4A). Quantitative assessment of

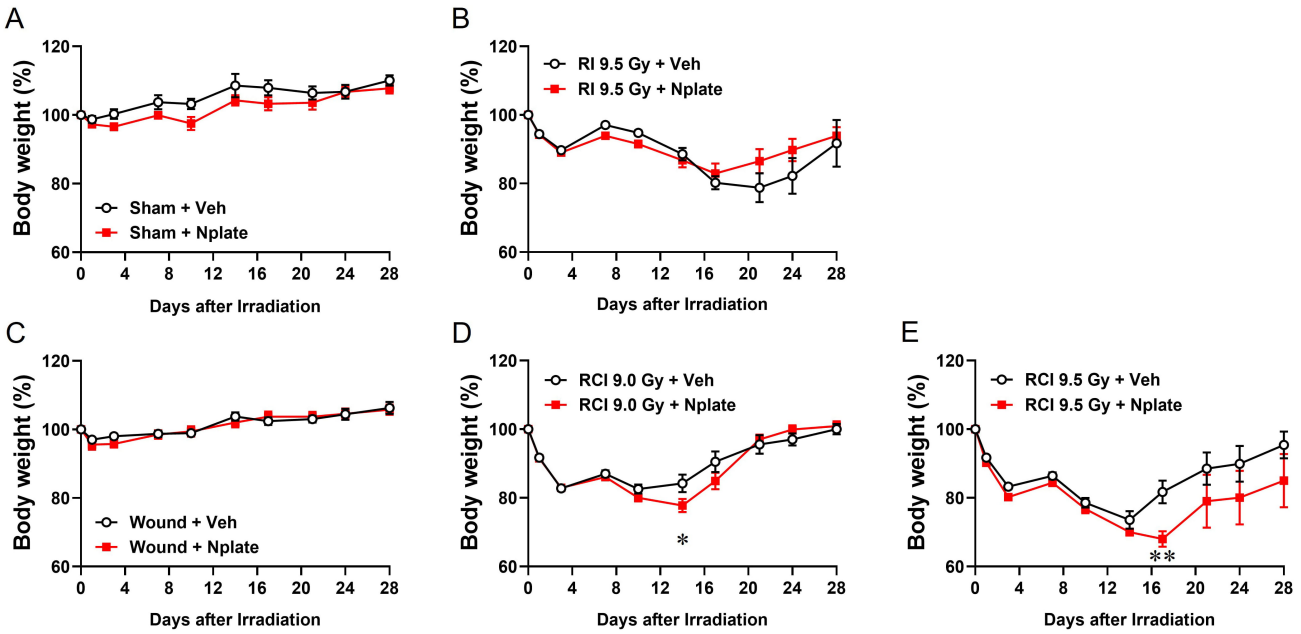

Fig. 2. Nplate exacerbates body weight loss after RCI. Body weight was monitored over 28 days and is expressed as a percentage of basal weight (Day 0, immediately after total body irradiation (TBI)) for vehicle-treated (black) and Nplate-treated (red) groups. (A,C) Non-irradiated controls: In Sham (A) and Wound-only (C) groups, Nplate treatment (30 µg/kg) had no adverse effects on body weight trajectories. (B) 9.5 Gy RI groups: After RI at 9.5 Gy, Nplate-treated mice exhibited a weight loss and recovery pattern similar to the vehicle control. (D) RCI groups at 9.0 Gy: Nplate treatment resulted in significantly greater body weight loss on Day 14 compared to the vehicle control (*p = 0.0211). (E) RCI groups at 9.5 Gy: The exacerbation of weight loss by Nplate was most pronounced on Day 17 (**p = 0.0036). Data are presented as mean ± standard error of the mean (SEM) (N = 3–20 per group with n = 3 in the RCI 9.5 Gy + Nplate group on day 28). Statistical significance between vehicle and Nplate groups was determined by two-way analysis of variance (ANOVA) followed by Šídák's multiple comparisons test.

megakaryocyte counts (Fig. 4B) and the percentage of adipocyte area (Fig. 4C) confirmed these findings. Specifically, Nplate treatment significantly suppressed adipocyte accumulation in the 9.5 Gy RI group (p = 0.0065). Furthermore, megakaryocyte counts in the 9.0 Gy RCI + Nplate group recovered to levels that were not significantly different from the Sham + Nplate or Wound + Nplate groups. It is worth noting that, within the vehicle treated groups, RI at 9.5 Gy induced significantly more adipocyte formation than RCI at 9.0 Gy (p = 0.0164) and at 9.5 Gy (p = 0.0013).

3.5 Nplate Treatment Enhances Haematopoietic Function on Day 30 After RCI at 9.0 Gy

To evaluate the impact of Nplate on functional haematopoietic recovery, we assessed the clonogenic potential of bone marrow cells on Day 30 post-TBI using CFU assay. As shown in Fig. 5, RI and RCI significantly suppressed the number of functional progenitor cells compared to Sham and Wound controls. However, Nplate treatment (30 µg/kg) significantly enhanced the recovery of multiple haematopoietic lineages across Sham, Wound-only and RCI groups. In the 9.0 Gy RCI group, Nplate-treated mice exhibited a significant increase in CFU-E (erythroid, Fig. 5B) and CFU-Total colony numbers (Fig. 5D) compared to their vehicle counterparts. This robust recovery was also shown in the Sham and Wound groups, where Nplate significantly bolstered colony formation across CFU-GM (Granulocyte, Macrophage, Fig. 5A), CFU-E (Fig. 5B), CFU-GEMM (Granulocyte, Erythroid, Macrophage, Megakaryocyte, Fig. 5C), or CFU-Total (Fig. 5D). While Nplate showed some positive trends in the 9.5 Gy RI and 9.5 Gy RCI group, the recovery was less pronounced and did not reach statistical significance in these groups. Collectively, these findings demonstrate that Nplate effectively promotes functional haematopoietic following RCI at 9.0 Gy.

3.6 Nplate Treatment Increases Peripheral Blood Cell Counts on Day 30 After RI at 9.5 Gy

To evaluate the impact of Nplate on systemic hematological recovery, peripheral blood cell counts were analyzed on Day 30 post-TBI across all experimental groups. As shown in Fig. 6, in the 9.5 Gy RI groups, Nplate treatment (30 µg/kg) significantly enhanced the recovery of leukocyte subsets, a significant increase in neutrophil (NEU) counts (Fig. 6B) compared to vehicle-treated RI controls (p = 0.0287). While total white blood cell (WBC, Fig. 6A), monocyte (MONO, Fig. 6D), and red blood cell (RBC, Fig. 6E) counts showed moderate trends to-

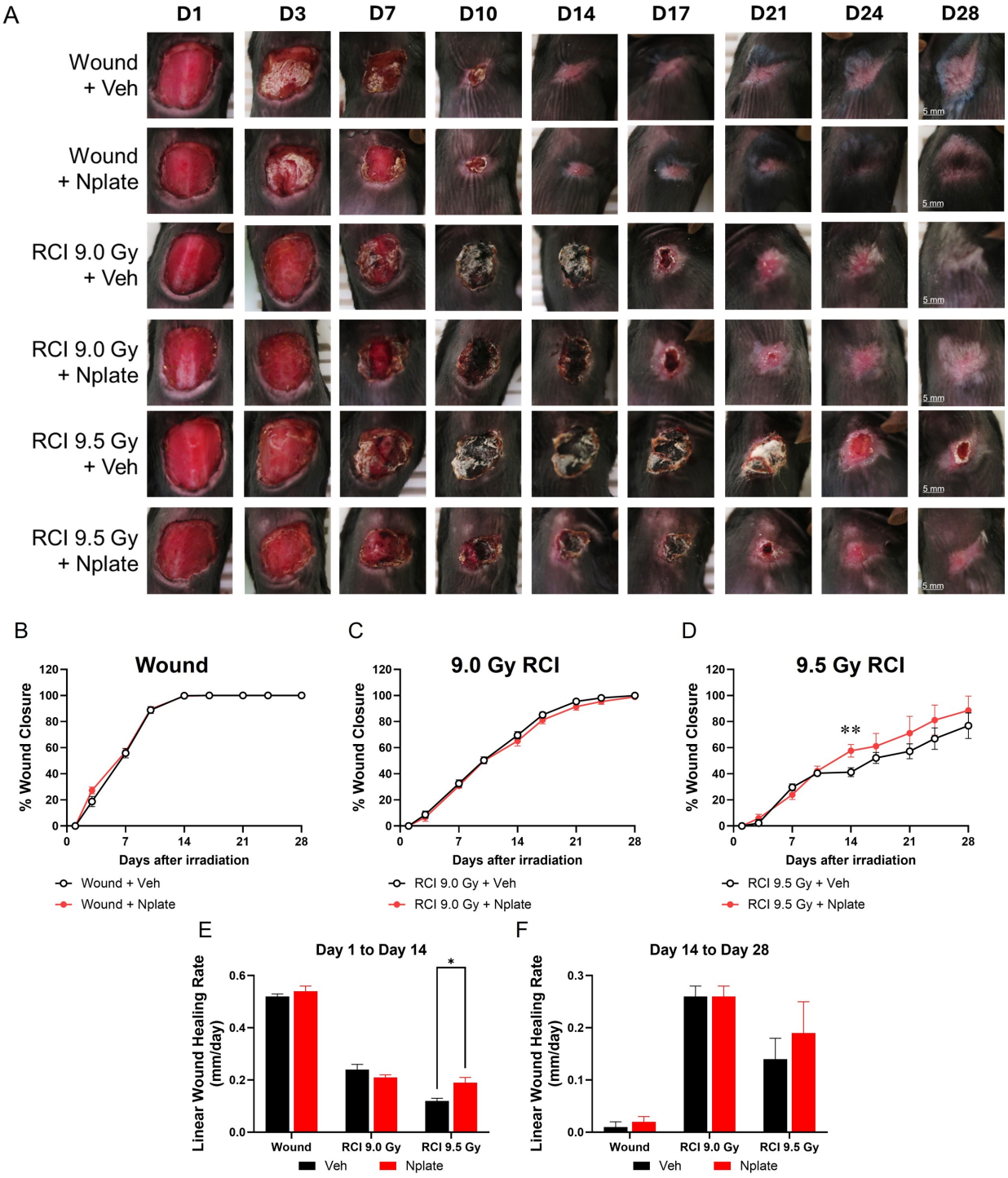

Fig. 3. Accelerated wound healing in RCI mice treated with Nplate after 9.5 Gy. Wound closure was monitored over 28 days and is expressed as a percentage of basal wound area (Day 1 post-TBI) for vehicle-treated (black) and Nplate-treated (red) groups. (A) Representative wound images from all wounded and RCI groups. Scale bar: 5 mm. (B) Wound groups and (C) RCI groups at 9.0 Gy: Mice in both groups showed no significant differences in healing rates between Nplate and vehicle treatments. (D) 9.5 Gy RCI groups: Nplate treatment significantly increased the wound closure on Day 14 (**$p = 0.0097$), compared to vehicle-treated controls. (E) Between Day 1 and Day 14, mice exposed to RCI at 9.5 Gy and treated with Nplate exhibited a significantly higher linear wound healing rate compared to vehicle-treated controls (*$p = 0.0205$). (F) Between Day 14 and Day 28, the linear wound healing rate showed no significant difference between Nplate and vehicle treatments across the Wound-only, 9.0 Gy RCI, and 9.5 Gy RCI groups. Data are presented as mean ± SEM (N = 3–20 per group with n = 3 in the RCI 9.5 Gy + Nplate group on day 28). Statistical analysis was performed using two-way ANOVA followed by Fisher's Least Significant Difference (LSD). Veh, vehicle; RCI, radiation combined injury.

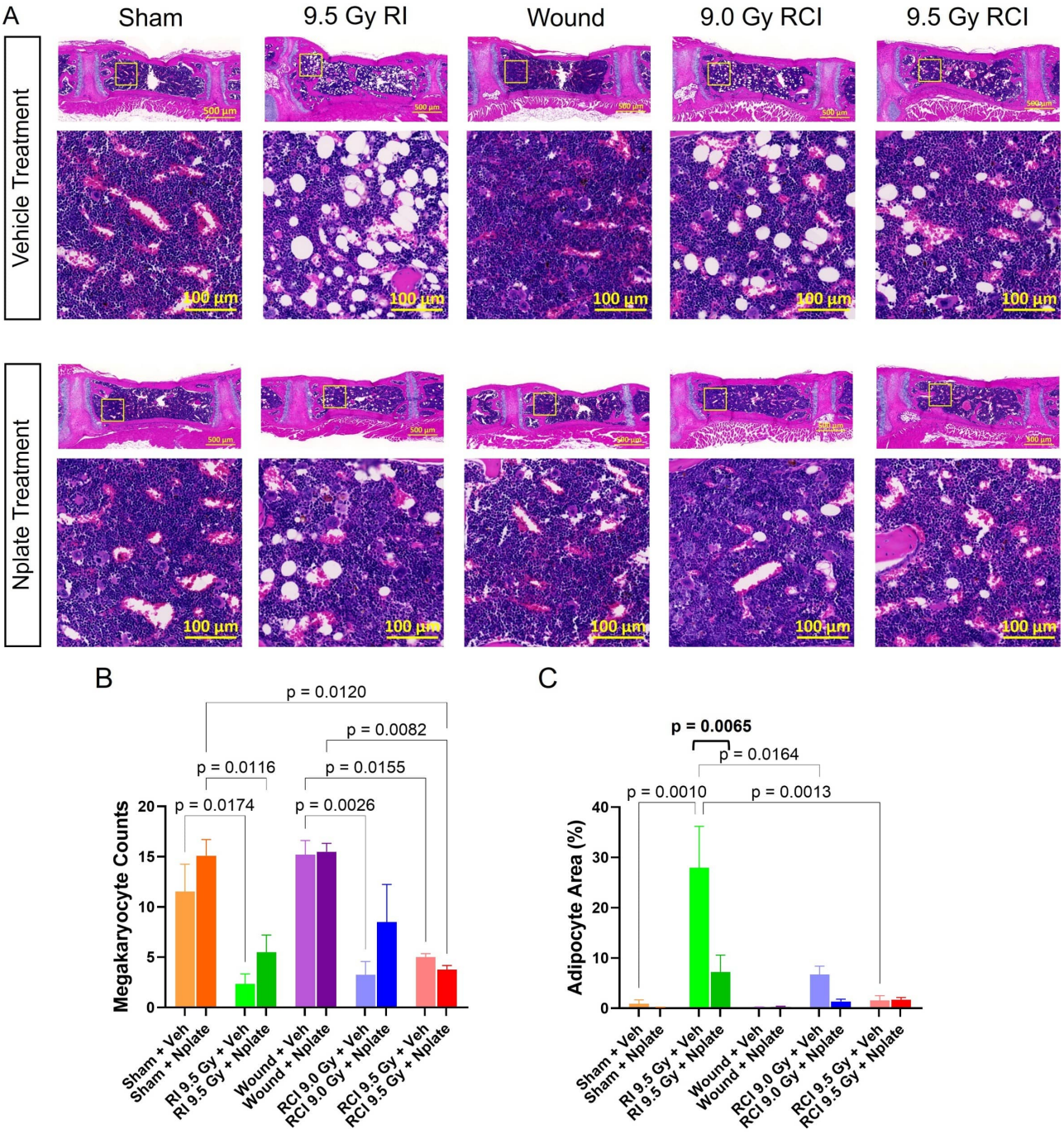

Fig. 4. Effects of Nplate on bone marrow hypocellularity after RI and RCI. Sternum bone marrow was harvested on Day 30 post-TBI for histological and quantitative analysis. (A) Representative Hematoxylin and Eosin (H&E) staining images: Top rows show low-magnification images (scale bar = 500 µm) with yellow insets indicating regions selected for high-magnification images (bottom rows, scale bar = 100 µm, area is approximately 130,000 µm^2). RI and RCI induced significant hypocellularity and adipocyte formation in vehicle-treated groups; conversely, Nplate treatment (30 µg/kg) resulted in denser haematopoietic clusters and reduced fatty marrow formation in both 9.5 Gy RI and 9.0 Gy RCI groups. (B) Megakaryocyte Counts: Quantitative assessment per 400× field revealed that radiation significantly reduced megakaryocyte counts in vehicle-treated groups. However, megakaryocyte counts in the 9.0 Gy RCI+Nplate group recovered to levels comparable to non-irradiated controls. (C) Percentage of Adipocyte Area: Measurement per 400× field showed that 9.5 Gy RI+Veh induced the highest adipocytes compared to Sham+Veh (p = 0.001), 9.0 Gy RCI+Veh (p = 0.0164), and 9.5 Gy RCI+Veh (p = 0.0013). Nplate significantly suppressed the percentage of adipocyte area in the 9.5 Gy RI group compared to its respective vehicle (p = 0.0065). Data are presented as mean ± SEM (N = 3–6 per group). Statistical significance was determined by one-way ANOVA followed by Tukey's multiple comparisons test. Veh, vehicle.

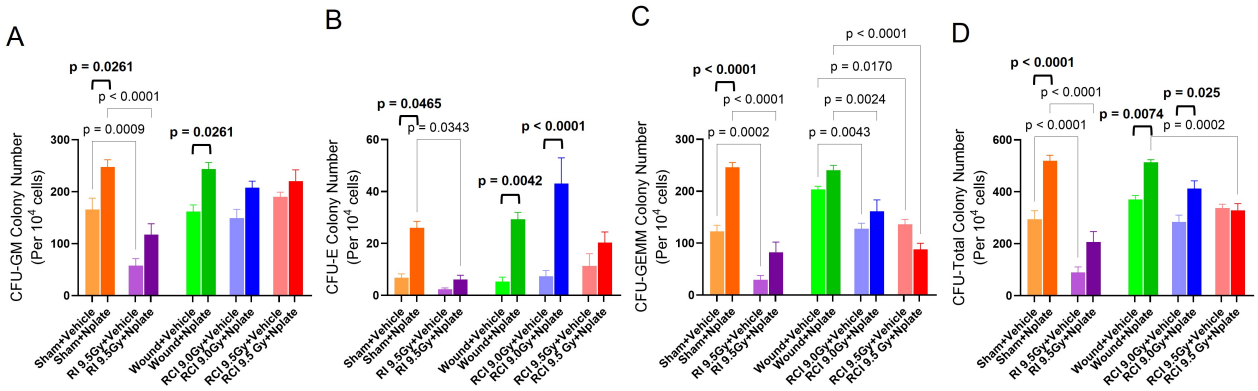

Fig. 5. Effect of Nplate on functional haematopoietic recovery after RI and RCI. Femurs were harvested on Day 30 post-TBI to assess the clonogenic potential of haematopoietic progenitor cells via CFU assays. (A) Colony forming unit–granulocyte, macrophage (CFU-GM): Nplate treatment (30 µg/kg) significantly increased the number of myeloid progenitors in Sham ($p = 0.0261$) and Wound ($p = 0.0261$) groups compared to their respective vehicle controls. (B) Colony-forming unit-erythroid (CFU-E): A significant increase in erythroid colonies was observed following Nplate administration in Sham ($p = 0.0465$), Wound ($p = 0.0042$), and 9.0 Gy RCI ($p < 0.0001$) groups. (C) Colony-forming unit—granulocyte, erythroid, macrophage, megakaryocyte (CFU-GEMM): Nplate significantly bolstered multipotent progenitor recovery in Sham ($p < 0.0001$) group only. (D) CFU-Total: Total colony counts were significantly higher in Nplate-treated mice across Sham ($p < 0.0001$), Wound ($p = 0.0074$), and 9.0 Gy RCI ($p = 0.025$) groups. Data are expressed as mean ± SEM (N = 6 per group). Statistical significance was determined by one-way ANOVA followed by Tukey's multiple comparisons test.

ward improvement in the RI + Nplate group, these measures did not reach statistical significance at this time point. In 9.0/9.5 Gy RCI, no significant differences were detected between Nplate- and vehicle-treated groups for any blood cell parameters. Lymphocyte (LYM) counts remained significantly suppressed across all irradiated groups compared to either Sham or Wound controls on day 30, regardless of treatment (Fig. 6C). Interestingly, a significant reduction in platelet (PLT) was observed in the Wound + Nplate group compared to the Wound + Vehicle group ($p = 0.0014$, Fig. 6F). Although the results showed a decrease in PLT counts in the sham group treated with Nplate and an increase in the RCI group at 9.5 Gy treated with Nplate, the data did not reach statistical significance (Fig. 6F). **Supplementary Table 1** listed the dataset of WBC, NEU, LYM, MONO, RBC. and PLT.

3.7 Nplate Stimulates the Recovery of the Splenic Lymphoid Compartment Following RI or RCI at 9.5 Gy

To evaluate the impact of Nplate on splenic recovery, we assessed spleen weight (Fig. 7B), splenocyte counts (Fig. 7C), and splenocyte density (Fig. 7D) 30 days post-TBI, with representative spleen images displayed in Fig. 7A. The RI-induced splenomegaly was displayed on the 2nd image of the vehicle group (Fig. 7A), but Nplate-treated RI group still showed splenomegaly (6th image of Fig. 7A). While RI and RCI significantly reduced total splenocyte counts and normalized splenocyte density compared to Sham and Wound controls, Nplate treatment (30 µg/kg) demonstrated a capacity to bolster lymphoid regeneration. In the RI group at 9.5 Gy, Nplate administration resulted in a 64% increase in splenocyte density compared to the vehicle-treated mice, and a similar restorative trend was observed following RCI at 9.5 Gy, which showed a 33% increase in normalized splenocyte density (Fig. 7D). However, these increases in density following RI and RCI at 9.5 Gy did not reach statistical significance, likely due to individual variations in response to radiation. Notably, the 9.0 Gy RCI + Vehicle group displayed significantly lower spleen weight compared to the 9.5 Gy RI + Vehicle group (Fig. 7B). Furthermore, Nplate treatment had no significant impact on spleen weight, splenocyte counts, or splenocyte density after RCI at 9.0 Gy (Fig. 7B–D). **Supplementary Table 2** listed splenic recovery data.

4. Discussion

This study demonstrated a divergence in the survival efficacy of Nplate when comparing RI to RCI. While Nplate served as a robust mitigator for RI, increasing 30-day survival by 45%, this therapeutic efficacy was completely abolished in the RCI groups, where the treatment appeared to exacerbate body weight loss. This finding aligns with our previous observations that certain established radiomitigators, such as pegylated granulocyte colony-stimulating factor (PEG-G-CSF), can be effective against RI but lose their survival-enhancing capabilities when radiation was combined with other traumas like burns or wounds [31]. Despite the absence of a survival improvement in the combined injury cohorts, Nplate provided significant regenerative advantages across multiple tissue compartments. Nplate treatment significantly accelerated acute wound healing, increasing the healing rate by 54% between Day 1 and Day

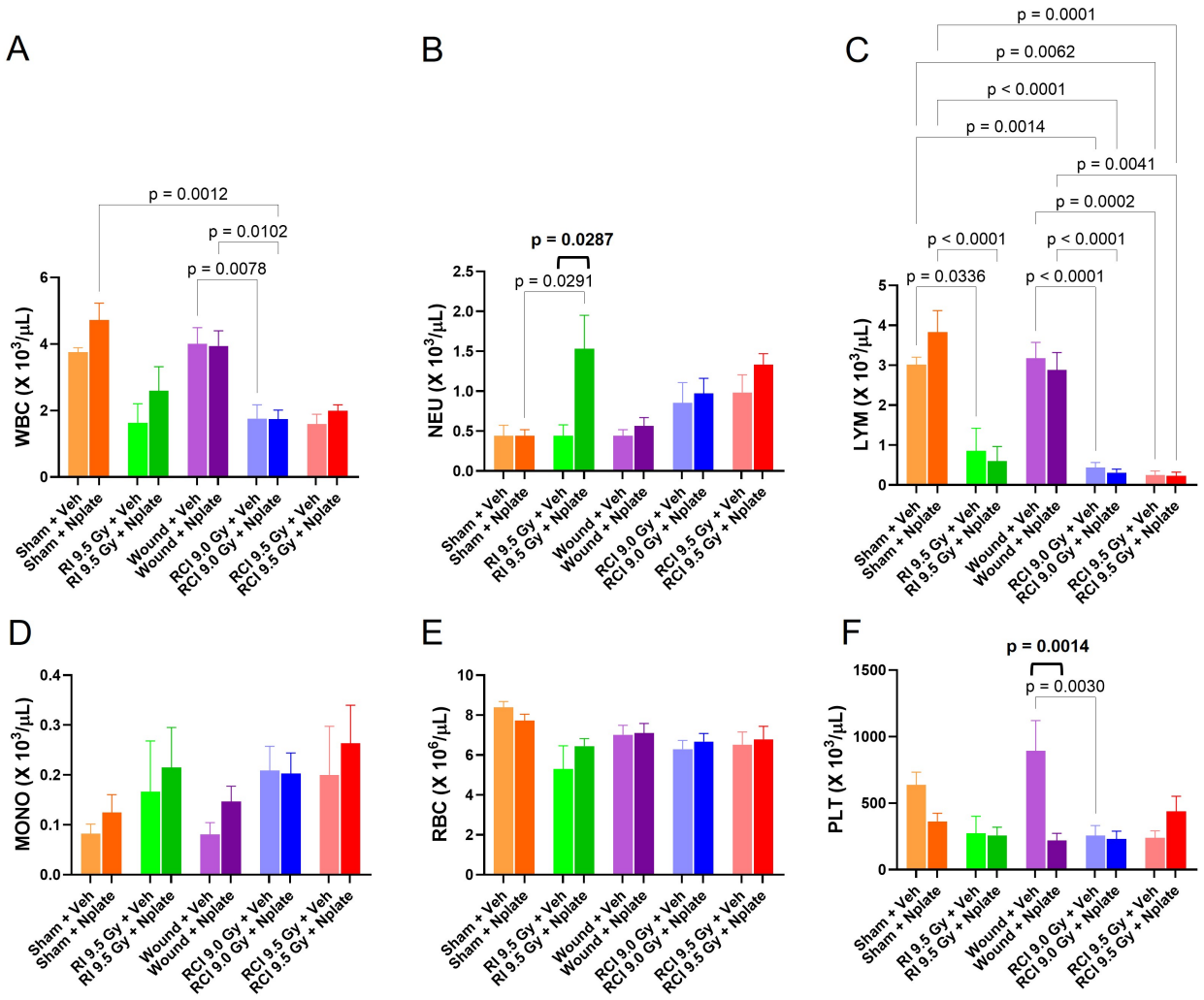

Fig. 6. Effect of Nplate on peripheral blood counts on Day 30 after RI and RCI. Peripheral blood was collected on day 30 post-TBI to evaluate systemic hematological recovery. (A) White Blood Cell (WBC) Counts: Radiation exposure induced a significant decrease in total WBCs compared to Sham and Wound-only controls. (B) Neutrophil (NEU) Counts: Nplate treatment (30 μg/kg) significantly enhanced neutrophil recovery in the RI group at 9.5 Gy compared to vehicle controls (p = 0.0287). (C) Lymphocyte (LYM) Counts: Significant lymphopenia persisted across all irradiated groups (RI and RCI) compared to Sham and Wound-only controls. (D) Monocyte (MONO) Counts: No significant differences were observed between treatment groups on Day 30 post-exposure. (E) Red Blood Cell (RBC) Counts: RBC levels remained stable across groups, with no significant impacts from radiation or Nplate treatment at this time point. (F) Platelet (PLT) Counts: Nplate treatment in the Wound + Nplate group resulted in a significant reduction in circulating platelets compared to the Wound + Vehicle group (p = 0.0014). Data are expressed as mean ± SEM (N = 3–10 per group). Statistical significance was determined by one-way ANOVA followed by Tukey's multiple comparisons test.

14. This local tissue repair was reflected by systemic improvements in the haematopoietic niche. Furthermore, Nplate demonstrated a positive trend toward lymphoid regeneration, increasing splenocyte density in the high-dose RI and RCI groups. While it may appear contradictory that Nplate promotes haematopoietic recovery without improving survival, this phenomenon is recognized as the "synergistic lethality" found in RCI. In RI, mortality is primarily driven by haematopoietic failure; thus, restoring cell counts typically rescues the animal. However, in RCI, the addition of a skin wound significantly alters the biological landscape: (i) While Nplate begins to reorganize the bone marrow and increase cell counts, the peak mortality window (Days 10–15) in RCI is also characterised by systemic inflammatory response exacerbated by the wound. Haematopoietic recovery alone may not be sufficient to overcome this systemic failure; (ii) The skin wound provides a portal for infection, and radiation-induced GI damage allows for bacterial translocation. Even if platelets and neutrophils are beginning to recover, they may be insufficient in number or function to prevent sepsis-driven mortality during that critical window.

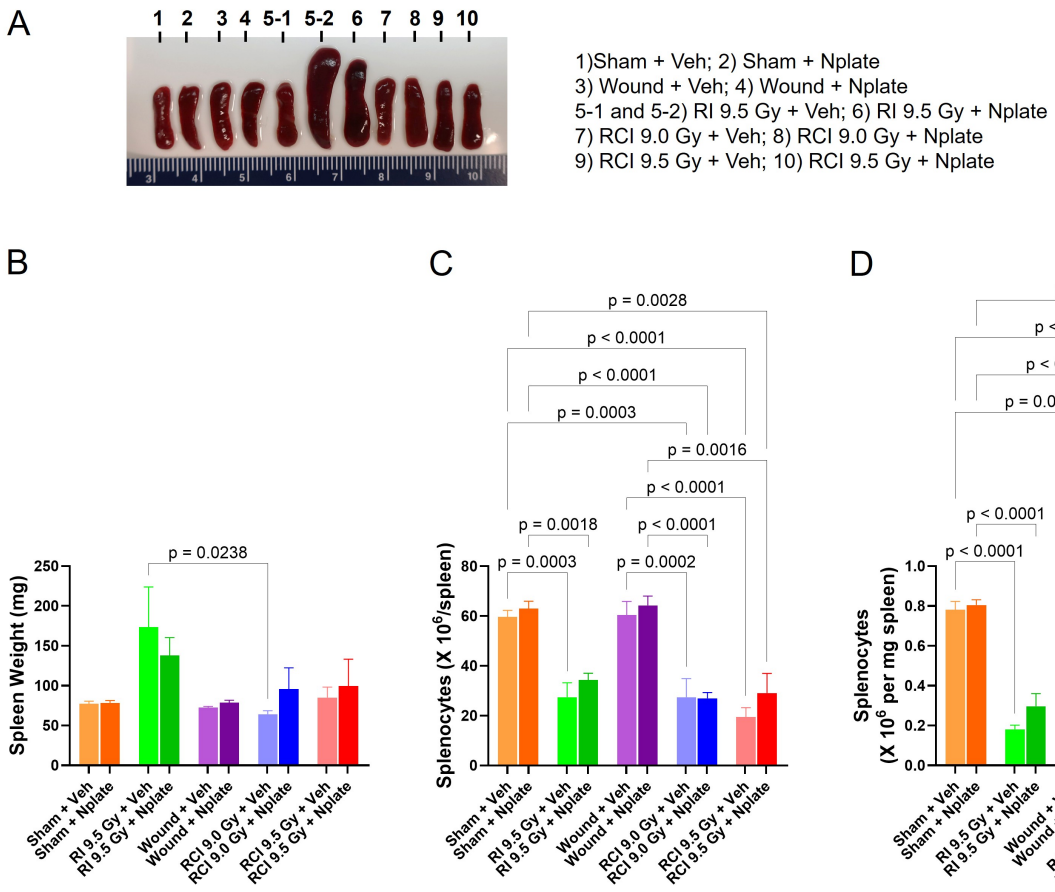

Fig. 7. Effects of Nplate on spleen weights, splenocyte counts, and splenocyte density after RI and RCI. Spleen was harvested on Day 30 post-TBI to evaluate splenic recovery across all experimental groups. (A) Representative Spleen Images: Visual comparison of spleen size across treatment groups: (1) Sham + Veh; (2) Sham + Nplate; (3) Wound + Veh; (4) Wound + Nplate; (5-1 and 5-2) RI 9.5 Gy + Veh; (6) RI 9.5 Gy + Nplate; (7) RCI 9.0 Gy + Veh; (8) RCI 9.0 Gy + Nplate; (9) RCI 9.5 Gy + Veh; 10) RCI 9.5 Gy + Nplate. (B) Spleen Weight: Quantification of total spleen mass (mg) on day 30. Radiation exposure generally increases spleen weight on day 30, with the 9.0 Gy RCI + Vehicle group displaying significantly lower weight compared to the 9.5 Gy RI + Vehicle group ($p = 0.0238$). (C) Splenocyte Counts: Total number of splenocytes ($\times 10^6$ per spleen). RI and RCI significantly decreased total splenocyte counts compared to Sham and Wound-only controls. (D) Splenocyte Density: Normalized splenocyte counts per mg of spleen tissue ($\times 10^6$ per mg). Nplate treatment (30 µg/kg) demonstrated a capacity to bolster regeneration, resulting in a 64% increase in density in the 9.5 Gy RI group and a 33% increase in the 9.5 Gy RCI group compared to their respective vehicle controls. However, these trends did not reach statistical significance. Data are expressed as mean ± SEM (N = 3–6 per group). Statistical significance was determined by one-way ANOVA followed by Tukey's multiple comparisons test.

The result that Nplate treatment significantly accelerated acute wound healing in the 9.5 Gy RCI group between Day 1 and Day 14 was particularly critical during the initial inflammatory and proliferative phases of repair, as evidenced by a significant increase in the percentage of wound closure on Day 14 compared to vehicle-treated controls. The magnitude of this effect may depend on the radiation dose and the severity of the underlying haematopoietic suppression. We attribute the difference in results between 9.0 Gy RCI and 9.5 Gy RCI to the following factors: (i) At 9.0 Gy RCI, the baseline physiological damage was less severe than at 9.5 Gy. The natural healing capacity of the 9.0 Gy group was relatively robust, leaving a smaller window for therapeutic improvement. In contrast, the 9.5 Gy dose induced more profound haematopoietic depletion and systemic stress, which significantly hindered natural wound closure. It was in this extreme environment that the mitigative effect of Nplate became statistically evident and biologically significant; (ii) The 0.5 Gy difference between 9.0 and 9.5 Gy represented a critical threshold in the RCI mouse model, moving from a lethal to a highly lethal injury. Our results demonstrate that Nplate may be particularly effective as a "rescue" agent under scenarios of extreme radiation stress. In contrast, a previous study using the TPO receptor agonist Alxn4100TPO reported a starkly different outcome, stating that the agent lacks the capabil-

ity to accelerate wound healing [31]. In that study, RCI at 9.5 Gy delayed healing by approximately 14 days, and the administration of Alxn4100TPO alone actually resulted in RCI wounds taking longer than 28 days to fully heal. This delay was further compounded when Alxn4100TPO was combined with other treatments like peg-G-CSF, which also failed to accelerate the wound-healing rate [31]. The divergent results observed between this study using Nplate and the research involving Alxn4100TPO highlighted significant pharmacological and structural nuances in how these agonists modulate the RCI manifestation. Nplate consists of TPO-binding peptides fused to an IgG1 Fc domain [32]. This specific structure may facilitate more efficient localized delivery or trigger a more robust signaling cascade that activates the early "angiogenic switch" and myofibroblast activity necessary for acute wound contraction. Conversely, Alxn4100TPO is characterized as a short-chain peptide incorporated into both the light and heavy chains of human IgG [33]. Despite its potency in the haematopoietic compartment, it lacks the capability to accelerate cutaneous wound healing [31]. This suggests that Alxn4100TPO signaling may be more sequestered within the bone marrow and spleen, whereas Nplate may exert a more profound influence on the paracrine environment of the cutaneous wound, potentially by mobilizing growth factors or progenitor cells essential for dermal repair. Nevertheless, Nplate-induced accelerated kinetic in wound healing was phase-specific. While Nplate-treated mice closed their wounds much faster during the first two weeks, there were no significant differences in the linear healing rate during the late remodeling phase. However, Nplate treatment did not improve the survival of RCI mice while Alxn4100TPO did [34], suggesting that survival improvement after RCI needs multi-organ participation in repairs other than wound healing acceleration.

Consistent with previous studies [17,18,19,35], the role of Nplate in haematopoietic recovery was supported by both structural and functional data from this study, demonstrating its ability to reorganize and revitalize the bone marrow niche following lethal-dose RI and RCI. We acknowledged that the recovery patterns varied across radiation doses in the RCI setting. However, the collective data support the conclusion that Nplate promotes haematopoietic recovery in RCI mice for the following reasons: (i) In 9.0 Gy RCI mice, we observed a significant depletion of megakaryocyte counts in the "RCI 9.0 Gy + Veh" group compared to "Wound + Veh" controls. Notably, this significant difference was abolished in the Nplate-treated groups; megakaryocyte counts in "RCI 9.0 Gy + Nplate" were statistically indistinguishable from "Wound + Nplate" controls (Fig. 4B). This indicated that Nplate restored the megakaryocyte population to near-normal levels despite the RCI; (ii) The functional improvement is further evidenced by the significant increase in CFU-E (Fig. 5B) and CFU-Total (Fig. 5D) colony numbers in the Nplate-treated RCI group at 9.0 Gy compared to its respective vehicle control. This demonstrated that Nplate directly enhanced the proliferative capacity of surviving progenitor cells in the RCI environment; (iii) It was important to note that all haematological and bone marrow data were collected from surviving animals on Day 30. In the 9.5 Gy RCI groups, survival was extremely low (~15–20%). This high mortality created a "survival bias" where the few remaining animals in the vehicle group were those with the highest natural resilience, making it statistically difficult to show a further "increase" in peripheral blood counts at that specific time point. Representative H&E staining demonstrated that Nplate-treated mice in the 9.5 Gy RI group possessed significantly denser haematopoietic clusters compared to their respective vehicle controls. Nplate treatment significantly suppressed the percentage of adipocyte area in this group. This functional boost was further reflected in the peripheral blood of survivors after 9.5 Gy RI, where Nplate administration led to a significant increase in NEU counts. Beyond its primary myeloid and erythroid effects, Nplate demonstrated a notable capacity for lymphoid regeneration, characterized by a 64% increase in splenocyte density in the 9.5 Gy RI group and a 33% increase in the 9.5 Gy RCI group. While these density improvements did not reach statistical significance, likely due to high individual variation in radiation response, the consistent upward trend depicted in both the 9.5 Gy RI and RCI groups suggests a broader immunomodulatory role of Nplate playing in the recovery of lymphoid organs.

These findings align with previous reports using the thrombopoietin receptor agonist Alxn4100TPO, which similarly increased megakaryocyte counts and significantly reduced fat cell counts in the bone marrow of both RI and RCI groups [31]. Furthermore, our observation that Nplate increased CFU-E and CFU-Total numbers in the RCI mice after 9.0 Gy is consistent with reports that Alxn4100TPO treatment can fully recover RBC counts, hemoglobin levels, and hematocrit readings [31]. The significant increase in NEU counts observed in the RI group after 9.5 Gy following Nplate treatment is also consistent with established data showing that TPO receptor agonists alleviated severe neutropenia and promoted multi-lineage haematopoietic recovery [31,36,37]. Interestingly, peripheral blood analysis revealed a paradoxical reduction in circulating platelets in the Wound + Nplate group compared to the Wound + Vehicle controls. This phenomenon likely reflected a complex feedback mechanism where, in the absence of radiation-induced bone marrow depletion, platelets were rapidly sequestered or utilized at the wound site to facilitate the wound healing [38,39]. Our observation in lymphoid recovery aligns with previous findings, which established that TPO receptor agonists like Alxn4100TPO can effectively alleviate lymphopenia and enhance the recovery of immune-related bone marrow cells. Specifically, Alxn4100TPO has been shown to significantly mitigate lymphocyte depletion in peripheral blood following 9.5 Gy irradiation, providing critical sup-

port for the restoration of the systemic immune compartment [31]. Furthermore, the reported ability of TPO receptor activation to alleviate neutropenia and promote the recovery of immature bone marrow cells suggests that the lymphoid recovery observed with Nplate may be part of a coordinated, multi-lineage reconstitution of the immune system following high-dose radiation exposure [31].

Collectively, these findings demonstrate that Nplate acts as a potent stimulator of multi-lineage haematopoietic and lymphoid recovery after RI and RCI. However, the failure to translate these demonstrable cellular and organ-level improvements into a significant survival enhancement from RCI remains a critical conundrum and suggests that the lethal synergy of RCI is driven by complex pathophysiological factors that extend well beyond primary haematopoietic failure. The exacerbated morbidity observed in the RCI groups, characterized by more pronounced body weight loss and accelerated mortality, is highly likely influenced by a cascade of severe systemic inflammation, profound endothelial dysfunction, and a compromised intestinal barrier [3,5,8,26,27]. Recent study in a murine RCI model (RCI + burn) have demonstrated a profoundly dysregulated inflammatory response, characterized by significantly elevated levels of pro-inflammatory cytokines such as IL-6 and altered tumor necrosis factor-alpha (TNF-α) signaling [40]. This systemic turmoil can lead to rapid-onset sepsis and multiple organ dysfunction syndrome, which, as observed in our results and the previous work, may not be fully mitigated by haematopoietic recovery alone [7,31,41]. Consequently, future therapeutic strategies for RCI may require a multi-modal approach, potentially combining Nplate with additional agents that specifically target inflammation, vascular integrity and/or gut barrier function to overcome the synergistic lethality of RCI.

5. Limitations

While this study provides significant insights into the regenerative potential of Nplate following RCI, several limitations must be acknowledged. First, the experimental group consisted exclusively of female mice. Given known sex-dependent differences in radiation sensitivity [42,43], future studies should include male mice to determine if these findings are sexually dimorphic. Second, this study evaluated only a single dose of Nplate (30 μg/kg) administered at a single time point (24 hours post-IR). While this dose proved effective for RI, it remains unclear whether a higher dose or a repeated-dosing regimen would be required to overcome the synergistic lethality of RCI. The pharmacokinetics of Nplate may be altered by the systemic stress associated with RCI, necessitating further dose-optimization studies. Third, our analysis was restricted to acute outcomes (30-day survival and recovery). While Nplate successfully stimulated early haematopoietic regeneration and wound healing, long-term studies will be needed to assess delayed effects, such as tissue fibrosis. Fourth, this study was primarily designed as a 30-day survival and mitigation efficacy study. Per the approved experimental protocol and IACUC requirements for survival studies, tissue collection was restricted to the final study endpoint on Day 30. By Day 30, most wounds in all groups had achieved full or near-full closure, reaching the remodeling phase. Therefore, histological analysis or molecular marker quantification at this stage would not accurately capture the dynamic inflammatory and proliferative changes that drove the 54% acceleration observed during the acute phase (Days 1–14). While we agree that earlier time-point skin tissue collection (e.g., Day 7 or Day 14) would provide valuable mechanistic insights, the original study design was focused on non-invasive longitudinal measurements to avoid the possible interference with the 30-day survival study. Finally, the inability of Nplate to improve survival in the RCI mice, despite its cellular improvement, suggests that targeting the haematopoietic system alone may be insufficient. Future research should explore multi-modal therapeutic approaches, combining Nplate with other medical countermeasures, such as antibiotics to manage secondary infections, or GI-protective agents, to address the multi-organ failure characteristic of RCI.

6. Conclusions

This study demonstrates that while Nplate is a highly effective medical countermeasure for H-ARS, its ability to improve 30-day survival is abolished in the presence of a skin wound. Although Nplate treatment failed to mitigate the synergistic lethality of RCI, it provided significant local and systemic improvement, including accelerated acute wound closure and enhanced bone marrow cellularity. Furthermore, Nplate effectively promoted functional haematopoietic and increased the recovery of the splenic lymphoid compartment following both RI and RCI. These findings suggest that Nplate is a potent stimulator of multi-organ regeneration. However, for the effective treatment of RCI, it may need to be integrated into a multi-modal therapeutic regimen. Such a strategy should concurrently address the severe systemic inflammation, endothelial dysfunction, and intestinal barrier disruption that characterize the complex pathophysiology of RCI.

Abbreviations

AAALAC, association for assessment and accreditation of laboratory animal care; AFRRI, armed forces radiobiology research institute; ANOVA, analysis of variance; CBC, complete blood count; CFU, colony-forming unit; CFU-E, colony-forming unit-erythroid; CFU-GEMM, colony-forming unit—granulocyte, erythroid, macrophage, megakaryocyte; CFU-GM, colony forming unit–granulocyte, macrophage; DLAR, department of laboratory animal resources; GI, gastrointestinal; H&E, hematoxylin and eosin; H-ARS, haematopoietic acute radiation

syndrome; IACUC, institutional animal care and use committee; IR, ionizing radiation; $LD_{50/30}$, lethal dose of radiation expected to cause death in 50% of an exposed population within 30 days; LYM, lymphocyte; MCM, medical countermeasure; MONO, monocyte; NCEA, nonclinical evaluation agreement; NEU, neutrophil; NHP, non-human primate; PDGF, platelet-derived growth factor; PLT, platelet; RBC, red blood cell; RCI, radiation combined injury; RI, radiation injury; SC, subcutaneous; SEM, standard error of the mean; TBI, total body irradiation; TPO, thrombopoietin; USUHS, uniformed services university of the health sciences; Veh, vehicle; WBC, white blood cell.

Availability of Data and Materials

The datasets used and analyzed during the current study are available from the corresponding author upon reasonable request.

Author Contributions

MX, JGK, and LW designed the research study. LW, BL, MZ, WC, LH, AZ, GC, MX, and JGK performed the research. JGK, LW, BL, MZ analyzed the data. LW wrote the manuscript. All authors contributed to editorial changes in the manuscript. All authors read and approved the final manuscript. All authors have participated sufficiently in the work and agreed to be accountable for all aspects of the work.

Ethics Approval and Consent to Participate

The animal study protocol was approved by the Institutional Animal Care and Use Committee of the Uniformed Services University of the Health Sciences (protocol number: AFR-20-021 and date of approval: 10 April 2020). All animal experiments and care protocols were conducted in strict accordance with the authoritative guidelines outlined in the National Institutes of Health (NIH) Guide for the Care and Use of Laboratory Animals. Furthermore, the study was carried out in accordance with the ARRIVE guidelines.

Acknowledgment

We gratefully acknowledge Mr. Asher Rothstein of the AFRRI for his expert assistance in proofreading and editing this manuscript.

Funding

This research was funded by NIH/NIAID/AFRRI Interagency Agreement (IAA) (grant number AAI26003-001-00000) and AFRRI intramural grant (grant number AFR-B2-13613).

Conflicts of Interest

The authors declare no conflicts of interest. Although "Henry M Jackson Foundation for the Advancement of Military Medicine, Inc., Bethesda" is a not-for-profit entity, there is no conflict of interest between this study and the institution.

Declaration of AI and AI-Assisted Technologies in the Writing Process

During the preparation of this work the authors used Google Gemini to check spelling and grammar. After using this tool, the authors reviewed and edited the content as needed and took full responsibility for the content of the publication.

Supplementary Material

Supplementary material associated with this article can be found, in the online version, at https://doi.org/10.31083/FBL52437.

References

[1] Wu W, Wu Y, Yang Z, Chen M, Hu J, Qu K, et al. Radiation-induced intestinal injury: from molecular mechanisms to clinical translation. Oncology Reviews. 2025; 19: 1613704. https://doi.org/10.3389/or.2025.1613704

[2] Zhang Y, Chen X, Wang X, Chen J, Du C, Wang J, et al. Insights into ionizing radiation-induced bone marrow hematopoietic stem cell injury. Stem Cell Research & Therapy. 2024; 15: 222. https://doi.org/10.1186/s13287-024-03853-7

[3] DiCarlo AL, Ramakrishnan N, Hatchett RJ. Radiation combined injury: overview of NIAID research. Health Physics. 2010; 98: 863–867. https://doi.org/10.1097/HP.0b013e3181a6ee32

[4] Messerschmidt O. Combined effects of radiation and trauma. Advances in Space Research : the Official Journal of the Committee on Space Research (COSPAR). 1989; 9: 197–201. https://doi.org/10.1016/0273-1177(89)90438-9

[5] Ledney GD, Elliott TB, Moore MM. Modulation of mortality by tissue trauma and sepsis in mice after radiation injury. (AFRRI Special Report No. 92-18). Bethesda, MD: Armed Forces Radiobiology Research Institute. 1992.

[6] U.S. Department of Health and Human Services. Radiation Emergency Medical Management (REMM). Combined Injury. 2024. Available at: https://remm.hhs.gov/radtrauma.htm (Accessed: 3 May 2026).

[7] Hay Q, Jennings R, Creel A, Gaffney K, Wagner C, Maxwell K, et al. Mathematical modeling of the combined effects of thermal burn and local irradiation. PloS One. 2026; 21: e0341595. https://doi.org/10.1371/journal.pone.0341595

[8] Wang L, Lin B, Zhai M, Hull L, Cui W, Xiao M. Endothelial Dysfunction and Impaired Wound Healing Following Radiation Combined Skin Wound Injury. International Journal of Molecular Sciences. 2024; 25: 12498. https://doi.org/10.3390/ijms252312498

[9] Kiang JG, Jiao W, Cary LH, Mog SR, Elliott TB, Pellmar TC, et al. Wound trauma increases radiation-induced mortality by activation of iNOS pathway and elevation of cytokine concentrations and bacterial infection. Radiation Research. 2010; 173: 319–332. https://doi.org/10.1667/RR1892.1

[10] Ince C, Mayeux PR, Nguyen T, Gomez H, Kellum JA, Ospina-Tascón GA, et al. THE ENDOTHELIUM IN SEPSIS. Shock (Augusta, Ga.). 2016; 45: 259–270. https://doi.org/10.1097/SHK.0000000000000473

[11] Tang F, Zhao XL, Xu LY, Zhang JN, Ao H, Peng C. Endothelial dysfunction: Pathophysiology and therapeutic targets for sepsis-induced multiple organ dysfunction syndrome. Biomedicine &

Pharmacotherapy = Biomedecine & Pharmacotherapie. 2024; 178: 117180. https://doi.org/10.1016/j.biopha.2024.117180
[12] Wang Y, Guan QN, Zhang ZJ, Zhang YM. Interaction between endothelial injury and immune response in septic shock: from basic research to clinical applications. Frontiers in Physiology. 2025; 16: 1627008. https://doi.org/10.3389/fphys.2025.1627008
[13] DiCarlo AL, Maher C, Hick JL, Hanfling D, Dainiak N, Chao N, et al. Radiation injury after a nuclear detonation: medical consequences and the need for scarce resources allocation. Disaster Medicine and Public Health Preparedness. 2011; 5 Suppl 1: S32–44. https://doi.org/10.1001/dmp.2011.17
[14] Rojavin Y, Seamon MJ, Tripathi RS, Papadimos TJ, Galwankar S, Kman N, et al. Civilian nuclear incidents: An overview of historical, medical, and scientific aspects. Journal of Emergencies, Trauma, and Shock. 2011; 4: 260–272. https://doi.org/10.4103/0974-2700.82219
[15] Singh VK, Seed TM. Cutting-edge animal models for radiation combined injury drug development. Expert Opinion on Drug Discovery. 2025; 20: 1573–1588. https://doi.org/10.1080/17460441.2025.2584319
[16] Singh VK, Seed TM. An update on romiplostim for treatment of acute radiation syndrome. Drugs of Today (Barcelona, Spain: 1998). 2022; 58: 133–145. https://doi.org/10.1358/dot.2022.58.3.3367994
[17] Bunin DI, Bakke J, Green CE, Javitz HS, Fielden M, Chang PY. Romiplostim (Nplate®) as an effective radiation countermeasure to improve survival and platelet recovery in mice. International Journal of Radiation Biology. 2020; 96: 145–154. https://doi.org/10.1080/09553002.2019.1605465
[18] Yamaguchi M, Hirouchi T, Yokoyama K, Nishiyama A, Murakami S, Kashiwakura I. The thrombopoietin mimetic romiplostim leads to the complete rescue of mice exposed to lethal ionizing radiation. Scientific Reports. 2018; 8: 10659. https://doi.org/10.1038/s41598-018-29013-5
[19] Bunin DI, Javitz HS, Gahagen J, Bakke J, Lane JH, Andrews DA, et al. Survival and Hematologic Benefits of Romiplostim After Acute Radiation Exposure Supported FDA Approval Under the Animal Rule. International Journal of Radiation Oncology, Biology, Physics. 2023; 117: 705–717. https://doi.org/10.1016/j.ijrobp.2023.05.008
[20] Silverman TA, Shadiack AM, Hofmeyer KA, Cecere AE, Eisnor DL, Hoffman CM, et al. Blood product use for radiological/nuclear trauma: product development and US regulatory considerations. Trauma Surgery & Acute Care Open. 2024; 9: e001123. https://doi.org/10.1136/tsaco-2023-001123
[21] Bortolotti M, Pettine L, Zaninoni A, Croci GA, Barcellini W, Fattizzo B. Efficacy and Immunomodulating Properties of Eltrombopag in Aplastic Anemia following Autologous Stem Cell Transplant: Case Report and Review of the Literature. Pharmaceuticals (Basel, Switzerland). 2022; 15: 419. https://doi.org/10.3390/ph15040419
[22] Ghanima W, Cooper N, Rodeghiero F, Godeau B, Bussel JB. Thrombopoietin receptor agonists: ten years later. Haematologica. 2019; 104: 1112–1123. https://doi.org/10.3324/haematol.2018.212845
[23] Gómez-Almaguer D. Eltrombopag-based combination treatment for immune thrombocytopenia. Therapeutic Advances in Hematology. 2018; 9: 309–317. https://doi.org/10.1177/2040620718798798
[24] Alizadeh M, Momeny M, Khodadoust E, Mahmoudi SM, Abolghasemi-Dehaghani S, Zarrabi M, et al. Platelet-Rich Fibrin (PRF)-Polymer Composites for Wound Healing: Macromolecular Synergies, Structural Design, and Therapeutic Efficacy. ACS Applied Bio Materials. 2025; 8: 8449–8466. https://doi.org/10.1021/acsabm.5c01083
[25] Doi T, Hori T, Onuma T, Mizutani D, Ueda K, Enomoto Y, et al. Thrombopoietin and collagen in low doses cooperatively induce human platelet activation. Acute Medicine & Surgery. 2022; 9: e769. https://doi.org/10.1002/ams2.769
[26] Ledney GD, Stewart DA, Exum ED, Sheehy PA, et al. Skin wound-enhanced survival and myelocytopoiesis in mice after whole-body irradiation. *Acta radiologica*. Oncology. 1981; 20: 29–38. https://doi.org/10.3109/02841868109130187
[27] Wang L, Zhai M, Lin B, Cui W, Hull L, Li X, et al. PEG-G-CSF and L-Citrulline Combination Therapy for Mitigating Skin Wound Combined Radiation Injury in a Mouse Model. Radiation Research. 2021; 196: 113–127. https://doi.org/10.1667/RADE-20-00151.1
[28] Gilman T. Wound outcomes: the utility of surface measures. The International Journal of Lower Extremity Wounds. 2004; 3: 125–132. https://doi.org/10.1177/1534734604264419
[29] Gorin DR, Cordts PR, LaMorte WW, Manzoian JO. The influence of wound geometry on the measurement of wound healing rates in clinical trials. Journal of Vascular Surgery. 1996; 23: 524–528. https://doi.org/10.1016/s0741-5214(96)80021-8
[30] Kumar VP, Holmes-Hampton GP, Biswas S, Stone S, Sharma NK, Hritzo B, et al. Mitigation of total body irradiation-induced mortality and hematopoietic injury of mice by a thrombopoietin mimetic (JNJ-26366821). Scientific Reports. 2022; 12: 3485. https://doi.org/10.1038/s41598-022-07426-7
[31] Kiang JG, Zhai M, Bolduc DL, Smith JT, Anderson MN, Ho C, et al. Combined Therapy of Pegylated G-CSF and Alxn4100TPO Improves Survival and Mitigates Acute Radiation Syndrome after Whole-Body Ionizing Irradiation Alone and Followed by Wound Trauma. Radiation Research. 2017; 188: 476–490. https://doi.org/10.1667/RR14647.1
[32] Mytych DT, Park JK, Kim J, Barger TE, Boshier A, Jawa V, et al. Assessment of romiplostim immunogenicity in adult patients in clinical trials and in a global postmarketing registry. British Journal of Haematology. 2020; 190: 923–932. https://doi.org/10.1111/bjh.16658
[33] Satyamitra M, Lombardini E, Peng T, 3rd, Devore D, Graves J, 3rd Mullaney C, et al. Preliminary nonclinical toxicity, pharmacokinetics, and pharmacodynamics of ALXN4100TPO, a thrombopoietin receptor agonist, in CD2F1 mice. Radiation Research. 2013; 32: 100–112. https://doi.org/10.1177/1091581813482336
[34] Kiang JG, Zhai M, Liao PJ, Ho C, Gorbunov NV, Elliott TB. Thrombopoietin Receptor Agonist Mitigates Hematopoietic Radiation Syndrome and Improves Survival after Whole-Body Ionizing Irradiation Followed by Wound Trauma. Mediators of Inflammation. 2017; 2017: 7582079. https://doi.org/10.1155/2017/7582079
[35] Vercellino J, Małachowska B, Kulkarni S, Bell BI, Shajahan S, Shinoda K, et al. Thrombopoietin mimetic stimulates bone marrow vascular and stromal niches to mitigate acute radiation syndrome. Stem Cell Research & Therapy. 2024; 15: 123. https://doi.org/10.1186/s13287-024-03734-z
[36] Neelis KJ, Dubbelman YD, Qingliang L, Thomas GR, Eaton DL, Wagemaker G. Simultaneous administration of TPO and G-CSF after cytoreductive treatment of rhesus monkeys prevents thrombocytopenia, accelerates platelet and red cell reconstitution, alleviates neutropenia, and promotes the recovery of immature bone marrow cells. Experimental Hematology. 1997; 25: 1084–1093.
[37] Neelis KJ, Hartong SC, Egeland T, Thomas GR, Eaton DL, Wagemaker G. The efficacy of single-dose administration of thrombopoietin with coadministration of either granulocyte/macrophage or granulocyte colony-stimulating factor in myelosuppressed rhesus monkeys. Blood. 1997; 90: 2565–2573.

[38] Opneja A, Kapoor S, Stavrou EX. Contribution of platelets, the coagulation and fibrinolytic systems to cutaneous wound healing. Thrombosis Research. 2019; 179: 56–63. https://doi.org/10.1016/j.thromres.2019.05.001

[39] Locatelli L, Colciago A, Castiglioni S, Maier JA. Platelets in Wound Healing: What Happens in Space? Frontiers in Bioengineering and Biotechnology. 2021; 9: 716184. https://doi.org/10.3389/fbioe.2021.716184

[40] Kumar R, Sharma AK, Bajaj S, Kalonia A, Shaw P, Yashavarddhan MH, et al. Developing a Murine Model for Radiation Combined Burn Injury Through Preliminary Assessment of Hematopoietic and Inflammatory Mediators. Radiation Research. 2025; 204: 449–466. https://doi.org/10.1667/RADE-25-00002.1

[41] Williams JP, McBride WH. After the bomb drops: a new look at radiation-induced multiple organ dysfunction syndrome (MODS). International Journal of Radiation biology. 2011; 87: 851–868. https://doi.org/10.3109/09553002.2011.560996

[42] Holmes-Hampton GP, Soni DK, Kumar VP, Biswas S, Wuddie K, Biswas R, et al. Time- and sex-dependent delayed effects of acute radiation exposure manifest via miRNA dysregulation. iScience. 2024; 27: 108867. https://doi.org/10.1016/j.isci.2024.108867

[43] Krukowski K, Grue K, Frias ES, Pietrykowski J, Jones T, Nelson G, et al. Female mice are protected from space radiation-induced maladaptive responses. Brain, Behavior, and Immunity. 2018; 74: 106–120. https://doi.org/10.1016/j.bbi.2018.08.008